IET Electric Power Applications

Research Article

IET Journals
The Institution of Engineering and Technology

Axial flux switched reluctance machines: a comprehensive review of design and topologies

ISSN 1751-8660
Received on 5th May 2018
Revised 27th November 2018
Accepted on 3rd December 2018
E-First on 24th January 2019
doi: 10.1049/iet-epa.2018.5190
www.ietdl.org

Hossein Torkaman[1] ✉, *Aghil Ghaheri*[1], *Ali Keyhani*[2]

[1]*Faculty of Electrical Engineering, Shahid Beheshti University, A.C., Tehran, Iran*
[2]*Department of Electrical and Computer Engineering, Ohio State University, Ohio, USA*
✉ *E-mail: h_torkaman@sbu.ac.ir*

Abstract: Axial flux switched reluctance machines (AFSRMs) exhibit unique characteristics that specify their superiority over other topologies in specific applications. A number of researchers have studied the efficient design and constructed structures in different types of AFSRMs. Each of such studies seeks to produce a motor with improved characteristics. Here, a comprehensive study is performed in AFSRMs, including their design considerations, sizing equations and the structural changes. The sensitivity of parameters for efficient operation is investigated. Also, the comparisons among topologies are provided for each of the identified metrics. This study ends with a comparison summary, which shows the performance indices evaluation of different topologies to utilise in various applications.

1 Introduction

Axial flux switched reluctance machines (AFSRM) are new generation of switched reluctance machine (SRM) structures. Today, SRMs are used as industrial drives [1–3]. SRMs introduce unique features. They do not have coils, brushes or magnets on their rotor [4, 5]. They have low inertia and weight and thus fast acceleration. These motors are suitable for high speed, high temperature and low-cost applications [6, 7]. However, their fundamental shortcomings are high torque ripple, noise pollution, lack of self-driving ability and dependency on the converters [8–10]. SRMs can generally be categorised according to [5, 11–14] in Fig. 1 based on their motion and flux path. In this category, there

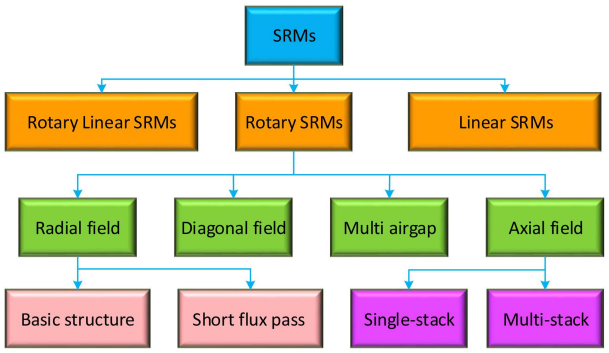

Fig. 1 *SRMs' classifications (from flux path and motion point of view)*

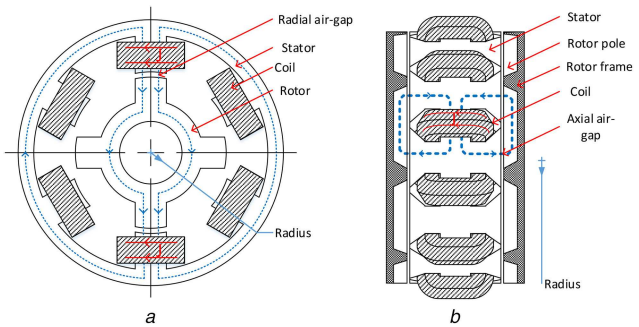

Fig. 2 *Two typical structures of SRM*
(a) RFSRM, ***(b)*** AFSRM

are four general types of SRMs. The initial classification is performed according to motion type offered by the machine: the rotary [11, 12, 15–19], linear [20–22] and rotary-linear [10, 14, 23–25]. The rotary machines are classified into four general types of 'axial flux', 'radial flux', 'diagonal flux' and a combination of all called 'multi-air-gap' according to position of the air-gap magnetic flux relative to the machine's rotation axis. The physical form of the axial flux and radial flux rotary SRMs is illustrated in Fig. 2. In this paper, focus is on AFSRMs.

Features: In this type of machines, the magnetic flux flows along the axial direction. In these machines, for specific volume, the active air-gap surface of the axial flux machines is larger compared to the radial flux type. In this type of motor, the flat shape of the structure causes the air-gap to be easily adjustable [26–28]. One of the disadvantages of the AFSRM is the construction of laminated cores. As an example, within the stator, the laminations of the yokes and the teeth are inserted in different directions [5, 29–31]. They are also made in different sizes so the stator cannot be made of multilayer laminations as in radial flux machines. However, the poles need to be laminated in the axial direction [32–34]. In addition, problems in assembling the two aforementioned parts and the difficult mechanical balance, especially in high powers, can be considered a weak point of this topology. In spite of the high copper losses in the axil flux machines with distributed windings, the AFSRMs normally have concentrated winding with a short end-winding, and in some structures, coils are arranged around the yoke (back to back), which results in a far smaller amount of losses.

Applications: Unique features of AFSRMs have made them highly functional in the propulsion industry such as utilisation like the in-wheel motors (IWMs) for electric vehicles [30, 32, 35–42], electrical powertrains [43], scooters [44, 45], microelectromechanical systems (MEMS) for semiconductor industries [46, 47], wind turbines [48] and simpler applications like fan [49]. Although for applications such an electric vehicle propulsion, there are some of the following limitations that can be solved to a target point: the torque density of the SRM is less than that of a competitors with magnets, which means that the machine may need more current for same power transmission. Also, SRM has a more intense vibration and noise ratio due to double saliency [50, 51]. According to outstanding features of the axial flux machines, almost all other types of custom radial flux machines such as induction wound synchronous [52], permanent magnet synchronous [53], doubly fed reluctance [54], variable reluctance

[55] and brushless DC type [56] can be implemented as the axial flux machines.

Problem description: In recent decades, researchers have paid much attention to AFPM machines [57, 58]. Regarding all the benefits, these machines are noticed significantly in the fields of electrical vehicles, transportation applications, astronavigation, aviation, paper industry, ships and submarines' propulsion and other industrial drivers [59–65]. AFSRM, unlike other radial flux machines, is able to compensate necessity of a cheap machine with acceptable characteristics in modern industries. That is how collecting assorted types of this motor can be so much beneficial as a complex. Many researchers have studied axial flux topologies before. As an example, in [66–68], a complete investigation of permanent magnet axial flux machines has been conducted, and different topologies with assorted combinations of rotor and stator poles are introduced and compared. Also in [69], history of AFIM is recounted, and subsequently, all topologies are investigated and evaluated. However, the SRMs, are only investigated in the radial flux (conventional) topology [70], and its assorted application in electric vehicles is discussed in [71–73]. Evaluation of the design of different topologies and assessment their features have not been investigated and compared in various applications so far. Therefore, this indicates the necessity of this study.

In this paper, the design procedure and evaluation of different topologies in the AFSRMs are discussed. It should be noted that the evaluating design criteria is important step for various applications [74]. In the following, some criteria and construction considerations in the design of AFSRMs are presented in Section 2. The basic design equations concerning this topology are expressed in Section 3, and a general design algorithm for a sample of AFSRM is presented. In Section 4, different existing topologies are introduced, categorised and their characteristics are discussed. Finally, in Section 5 a functional comparison is made, and efficiency, torque ripple, torque weight density and power volume density of all topologies are compared with one another.

2 Design and construction considerations in AFSRM

Some criteria and construction considerations in the design of electrical machines are the same. However, a number of features, such as magnetic materials used for forming the cores, non-magnetic materials for tightening the poles, stator coils structure, number of phases and the power limitation are more significant in AFSRMs which are discussed in this section.

Magnetic cores: Magnetic cores of stator, rotor and also rotor poles in the type of segmented AFSRM can be made of different materials including ferromagnetic iron with desired permeability [28–30, 32, 35, 36, 44, 46, 75–87], soft magnetic composite (SMC) [13, 88–90] and the constructed laminations from oriented electrical steel [91–93].

The cores of rotor and stator are exposed to alternating magnetic flux; special methods should be adopted to decrease the eddy currents. The stator cores are made in laminations to decrease the eddy current losses as much as possible and make the machine more efficient. The important issue here is the process of laminating the cores since, in axial flux machines, the cores cannot be formed by putting some similar laminations on each other simply. It is often constructed through rolling a silicone foil spirally and applying the slots on the resulted reel [32, 35, 81], but in [29] the stator poles are laminated in one direction separately, and the stator yoke in another direction.

In [13, 88–90], the electrical resistance of the cores is increased largely via forming the cores by soft magnetic powdered materials (composite-SMC-SLSMC), therefore, the eddy current losses have dropped more than before, however, this action brings up the serious weakness of decreasing average flux density of core. This is because of the magnetic composite materials and weaker *B–H* curves. It is due to relatively low permeability of the most commonly used SMC materials. Weak structural strength of powder in the core limits applicability of SMC under extensive loading condition. Shape of the core part has to be designed according to the mechanic loading and maximum allowable stresses in the material.

Using oriented electrical steel lamination reduces the hysteresis losses and therefore improves the efficiency. This utilisation is desirable only when material cost is not the design objective and does not impose an economic limitation. Using magnetic composite decreases the costs in milling and punching the laminations are not needed. However, the effective magnetic flux density decreases and the machine's size will increase. At constant power, the torque density will decrease. The process of laminating traditional non-oriented steels increases cost and complexity.

Frames: Selecting the non-magnetic materials as holder of the poles, the magnetic and the mechanical characteristics of the utilised materials are noticed. Poles' holding frames facilitate the use of a non-ferromagnetic material to construct the rotor or the stator structure. The rotor segments need to be magnetically insulated from one another in AFSSRMs and that these different parts have to be tightened in their specific positions, a non-magnetic frame is needed. In [35, 75, 77, 83, 94], Aluminium is utilised to achieve this objective, but in [36], compact plastic is used. The important issue in selecting these materials is the very low magnetic conductance coefficient and a very low weight density but high thermal conductance. In this way, not only the rotor segments get insulated but also the rotor inertia decreases and subsequently motor dynamic response increases. For better heat transfer of magnetic cores inserted in the disks which are considered heat sources and are in direct contact with surrounding environment, existence of a material with high heat transfer coefficient is important. Generally, it is desired to obtain a material with low magnetic permittivity which does not make an ineffective magnetic path and a high thermal conductivity that helps cooling the involved cores, in which the aluminium would be a proper candidate.

The stator coils structure: The stator windings of AFSRM are designed according to the design considerations and also the magnetic flux path. In the typical designs, the toroidal coils are wound around the stator poles [35, 92, 95]. In some simpler structures [96, 97], the stator cores are separate, and they are wound annularly, and the winding process may be applied automatically. In [40, 42, 95], a structural supporter is needed to maintain the stator poles which are made separately without a fixed yoke next to each other. The heat transfer is troubled in these structures in which the stator is surrounded by the rotors. In designing such structures, the slots' Ampere-turn ratio must be considered a small value.

The stator poles are divided into two general types, the main and the auxiliary one. The windings are placed on the main poles. This topology is presented as 'single teeth winding' or 'modular stator' [81, 85]. The simplest type of a winding is noticed when high turns of a thin conductor are used in coils. In this type, a topology like [82] solves the problem. In a multi-layer construction of a motor, each stack has only one coil that is prepared simply through an industrial process and placed in the considered position. In a specific condition, by wrapping the conductors around the stator yoke, the magnetic flux path gets too short. In [35], it is stated that in this condition, the stator yoke acts as a structural support and therefore, there is no need for a disk that carries the teeth and the stator windings. The other type that has received no attention on behalf of the designers is the high-temperature superconductive. It is suitable for motor with sandwiched stator that has no core. In this topology, the iron loss of the machine has decreased, and the torque density has been increased [98].

The number of the motor phases: AFSRM might include assorted phase numbers. In the single-phase type, number of stator and rotor poles are equal, i.e. poles ratio of the machine is one [49, 99]. That is why, if the rotor stops in the aligned position, it cannot start again by switching the coils. The permanent auxiliary magnets or asymmetrical pole shoes are used [5, 99] for proper operation. This motor can operate as multi-phase. The three-phase type is suitable since they do not have rotor lock problem unlike single phase type in symmetrical position; three-phase converters are also commonly used with appropriate costs and acceptable ripple [28, 36, 40, 83, 88, 100–103]. Interestingly, the topologies are designed

in four phases [37, 46, 104], five phases [105] and even six phases [82]. The most important problem of this topology is the necessity of more complicated drive systems and the wider utilisation of power electronic devices that leads to higher expenses and considerable switching losses. Nevertheless, the torque response of the machine gets smooth which results in slighter noise and longer lifetime of the machine [97]. However, in [82] it has been mentioned that in a six-phase topology, it is possible to use two common three-phase drivers and no extra converter is required, and the costs will be decreased. A two-phase topology has not ever been presented for AFSRM. However, it can be implemented, and the phases can be connected precisely according to structures of [106, 107].

Torque profile: To improve the torque ripple, some techniques can be utilised, including skewing the stator poles [36], increasing number of phases [77] and displacement of the adjacent poles in rotor [32]. The output torque per weight can be increased by rearranging the windings for better operation of AFSRM by utilising the segmented rotor structures as compared to the conventional structures with salient pole rotors [35, 103, 108]. Improving torque density and efficiency is possible by increasing the numbers of poles or rotor parts versus number of stator slots [32, 35, 42]. High number of the rotor poles decreases flux per pole which subsequently makes the motor compact via decreasing the passing part.

The motor power limitation: Some troubles like tough mechanical balance in high powers, regarding the output power relationship with the outer diameter of the machine, and uniform construction of the air-gap limits the machine's design. These issues limit the boundary of power in AFSRM [4, 83]. The special applications often determine the specific operation limitation of these machines. Generally, AFSRM designs are developed in power ranges from a few tenths [37, 44, 83] to several kilowatts [35, 36, 40, 77, 78, 85, 109, 110] in various applications such as electrical transportation. But special designs like electrical trains are in the range of tens of kilowatts [43] or the applications related to laboratories are presented in the limited range of a few watts [88, 111]. MEMS application is an exceptional case in which power is in micro-watt range; it is also the fastest and smallest AFSRM designed so far [46, 47]. It can be stated that these motors operate in a vast power range.

3 Design of AFSRM and the dimensional equations

Generally, behaviour of the output power of the electric machines is a function of the machine's outer diameter, stack length (the active axial length), special electrical loading, special magnetic loading and the rotor speed [112]. AFSRM equations were first presented using design equations of radial-flux switched reluctance motors (RFSRMs) [113] by the same author. In [113], the output power for RFSRM has been extracted. Using these extended equations and regarding the ideal supplying current and also knowing the inductance ratio of aligned to unaligned position, equation of the AFSRM power which contains two stators with U-shape cores and a rotor has been extracted. First, the voltage equation of this case is as follows:

$$V = rI_{\mathrm{r}} + \frac{\mathrm{d}}{\mathrm{d}t}(LI_{\mathrm{r}}) \tag{1}$$

$$V = rI_{\mathrm{r}} + \frac{\mathrm{d}L}{\mathrm{d}t}I_{\mathrm{r}} + \frac{\mathrm{d}I_{\mathrm{r}}}{\mathrm{d}t}L \tag{2}$$

in which I_{r} is value of the desired rated current, r and L are coil resistance and inductance of the stator, respectively. Ignoring the coil resistance and regarding constant current variations versus time if an ideal control method is employed, (2) turns into the following equation:

$$V = \frac{\mathrm{d}L}{\mathrm{d}t}I_{\mathrm{r}} \tag{3}$$

This equation can be extended as follows:

$$Vt_{\mathrm{t}} = I_{\mathrm{r}}[L_{\mathrm{a}} - L_{\mathrm{u}}] \tag{4}$$

in which L_{a} and L_{u} are aligned and unaligned inductances, respectively. Parameter t_{t} represents time that the rotor goes from unaligned position to the aligned position (transition period). ω_m is speed and the turning angle is β_s, therefore

$$t_{\mathrm{t}} = \frac{\beta_s}{\omega_m} \tag{5}$$

Also, the linkage flux $L_{\mathrm{a}}I_{\mathrm{r}}$ in the aligned moment leads to (6), the magnetic loading B and the cross-section surface of the pole A_{s} can be stated

$$L_{\mathrm{a}}I_{\mathrm{r}} = BA_{\mathrm{s}}N_{\mathrm{ph}} \tag{6}$$

in which N_{ph} is the number of turns in each phase. If ratio of the aligned to unaligned inductance is defined as (7) and also (5)–(7) are inserted into (4), then (8) is followed

$$\alpha = \frac{L_{\mathrm{a}}}{L_{\mathrm{u}}} \tag{7}$$

$$V = \left(1 - \frac{1}{\alpha}\right)\omega_m BN_{\mathrm{ph}}\frac{A_s}{\beta_s} \tag{8}$$

The power equation is defined as follows:

$$P = m\,\mathrm{DVI}_{\mathrm{r}} \tag{9}$$

in which η is efficiency and D is duty cycle and defined as

$$D = \frac{\theta_{\mathrm{c}}P_{\mathrm{r}}}{360}\frac{P_{\mathrm{s}}}{2} \tag{10}$$

in which θ_{c} is conductance angle in degrees and P_{s} and P_{r} are the number of poles in stator and rotor, respectively. By combining (8) and (10), the power equation is obtained as follows:

$$P = m\eta Dk_i BN_{\mathrm{ph}}\omega_m I_{\mathrm{r}}\frac{A_s}{\beta_s} \tag{11}$$

in which K_i is defined as

$$K_i = \left(1 - \frac{1}{\alpha}\right) \tag{12}$$

Finally, the power equation is briefly expressed as

$$P \propto BA_{\mathrm{sp}}V_{\mathrm{sp}}\omega_m \tag{13}$$

$$V_{\mathrm{sp}} \propto \left(D_{\mathrm{o}}^2 - D_{\mathrm{i}}^2\right) \tag{14}$$

in which V_{sp} is the machine's volume, D_{o} is the outer diameter and D_{i} is the internal diameter of the stator. The rest of design equations are calculated through the above equations according to the selected topology, and if necessary, they are optimised as functions of the specific objective functions that could be torque density or the efficiency.

Now, according to existence of various topologies and structural differences in designing AFSRM, a general algorithm can be presented in which the general dimension conditions like outer diameter and the axial length are specified (as an example, an application like IWM limits these parameters). The general design algorithm can be presented as illustrated in Fig. 3, where D_{i}, D_{o} and D_{av} are inner, outer and average diameter, respectively, L_{tot} is

summation of active axial lengths and L_m is a maximum axial length limit.

4 Different AFSRM classifications

Structurally, AFSRMs can be classified into various types of salient or segmented poles, higher or less than one ratio of the stator/rotor poles, back to back or drum winding, disk-shaped or none-disk shape types, with or without the radial field and with or without the auxiliary poles of the stator. A comprehensive classification of different types of AFSRMs has been illustrated in Fig. 4. AFSRMs may take advantage of a single-sided (SS) rotor and stator (single air-gap layer), double-sided (DS) rotor(s) and stator(s) (two air-gap layers), multi-stack (MS) or a structure of both axial and radial fluxes, integrated radial and double axial flux. In the following, studies that have focused on AFSRMs will be classified and analysed according to four main categories which have already been explained.

4.1 SS-AFSRM

The simplest AFSRM is made up of a stator and a rotor which are separated by an air-gap which is perpendicular to axis. The simpler type of this structure with toothed rotor (SST-AFSRM) is depicted in Fig. 5. The stator includes yoke, accommodated poles and the coils which wrap the poles as rings, concentrically. The stator core and the poles are all laminated. As explained in the introduction, the stator is made by rolling the tape shape laminations. The rotor is of ferromagnetic material and is made up of laminations. The density of power and torque is boosted compared to RFSRM. The problem of this topology is lack of uniform distribution of the applied forces between stator and rotor that will result in noises, warps, coil deformations, the bearing destruction and the possible collision of rotor poles and the stator. To reduce the axial forces, reduction of the excitation angle would be a solution.

In [109], a new solution for the core laminations has been proposed. Regarding the machine's magnetic flux paths in three dimensions, the yoke's and poles' laminations are needed in two different directions. The lamination process of SST-AFSRM is illustrated in Fig. 6. This process is too arduous, time consuming and needs high-tech equipment. This is regarded as shortcomings of this type of machines. In [81], the improved topology of SS-AFSRM with segmented rotor (SSS-AFSRM) has been presented. The stator is made up of a yoke and two series of main and auxiliary poles. The main poles are wound with the coils concentrically. The rotor consisted of a non-magnetic frame that holds the magnetic parts (Fig. 7).

The advantages of this topology are the copper loss reduction and the shortened path of the magnetic flux that has reduced iron loss and improved the power density. Also, inertia and weight of rotor have decreased due to installing the parts in an aluminium frame [103].

The problem of axial forces still exists in this topology. These forces might change symmetry of air-gaps, motor vibrations and increase torque ripple. Different mechanical structures are used to improve the axial force for designing two-stator motors [30, 94]. The schematic of magnetic path of this machine is illustrated in Fig. 8 in two positions of the poles' alignment and non-alignment. SMC materials are utilised in [88, 89, 114] to improve the SS SRMs economically. These materials can be implemented in various forms with considerably low electric permittivity coefficient of almost one thousandth of one solid steel. In this design, there is no need for laminating. Fig. 9 depicts a three-dimensional view of these machines [88]. Comparing the static and dynamic status, reduction of eddy currents is considerable to an extent that becomes almost negligible.

4.2 DS-AFSRM

DS-AFSRMs are classified into two general categories with respect to the rotor and stator positions. Each category consists of some subsets which differ according to physical form of stator, rotor type (segmented or salient pole) and ratio of number of the stator poles to rotor poles.

4.2.1 US-AFSRM: AFSRMs with U-shaped stators (US-AFSRM) have already been introduced in single phase [5, 99], single phase with modular poles [49] and multiple phases [44, 83, 110]. In the single-phase type, the separated U-shape stator poles have been installed on the outer space of the container disk, and an exciter round coil embraces the whole complex. The rotor is segmented and designed in two different structures with ┤ shape poles, [99], and I shape poles [5], which is put around the stator. The stator winding is supplied through a single-phase pulse. When the stator excitation gets disconnected, the rotor continues rotating due to its mechanical inertia until it gets closer to the stator poles until the stator excitation current gets connected again [99]. This is how the rotor keeps rotating by repeating the stator excitation. Fig. 10 shows the single-phase US-AFSRM. Best performance of the single-phase SRM is in duty cycle of 0.5. Therefore, it has a discrete torque along the torque ripple and loud noise. This motor can be appropriate for applications which are not sensitive to the aforementioned problems like handicrafts and household applications. However, in modular-poles topology, the stator is unified and includes poles with active U-shape surfaces installed on each other and retained by the stator yoke and the concentric coils that wrap the poles. The rotor is segmented such that the active surface of the poles is made up of some ┤ shape edges piled. This topology is very influential for increasing the aligned position inductance (maximum inductance). Increasing L_{max} improves efficiency and power density. However, the torque ripple limits their use solely to fan applications since the fans' inertia decreases torque ripple [49].

Structurally, the common three-phase US-AFSRM has two stator disks on the sides and a rotor disk surrounded by the stators [44, 83]. As it is shown in Fig. 11, each stator disk consists of three poles which are designed as U-shapes and tightened by an aluminium supporter. The stator poles of both disks precisely face each other and are aligned mechanically. The segmented rotor consists of only two circular tape-like poles with equal surfaces. The stator and rotor poles are tightened by non-magnetic materials like aluminium [83]. The confronting coils in two stators need to be excited by opposite polarity. The magnetic flux path of this topology is illustrated in Fig. 12. There are also higher phase number (e.g. 4) topologies which consist of multiple single phase US-AFSRM and categorised into MS-AFSRM category [110].

4.2.2 CS-AFSRM: C-shape stator core AFSRMs are classified into two categories. The first one is a five-phase 12/15 SRM which is in the category of axial flux motors and has influential features like high torque density, low level of vibration and the ability to control the torque ripple profile for use in electric vehicles [97]. A three-dimensional image of this machine is shown in Fig. 13. The stator of this machine is made up of 15 C-shape separate cores which are wound concentrically and fixed by the motor hub separately. The rotor has a disk shape which is surrounded by the stator. The rotor frame is constructed from a very low magnetic penetration material like aluminium. On the rotor disk, there are 12 square cavities in which 12 laminated iron cubes are installed [105].

In each 120 mechanical degrees, 5 cores are connected to the 5 phases. Hence, there are three sets of this structure so that the mechanical force gets better distributed on the motor topology [33]. In this topology, the electromagnetic force does not possess an axial factor. That is why the noise source has been removed or lowered to the greatest extent. The motion pitch can decrease as the rotor diameter increases since the magnetic loading is not a function of the rotor diameter and a reduction in ripple torque. However, it increases volume of the machine and decreases power density.

Also, by increasing the rotor diameter, the torque increases according to $\tau = F \times r$. The C-shape cores are separate. They are wound by automatic devices. Moreover, the lamination process of these sheets is easier and simple to implement, since all the sheets are alike. In this topology, the slot volume does not limit the winding process. The designer is free to design such that losses are minimised. In addition, maximum heat distribution and dissipation occurs since the coils are inserted in the outer parts [77]. The

author has presented a developed model for decreasing the fringing flux. As it is shown in Fig. 14, a wedge part has been created on the front edge that causes the fringing flux to pass a longer path. In this design, the reluctance path gets longer and ends up decreasing this undesired flux [33, 77]. The magnetic flux path of CS-AFSRM is illustrated in Fig. 14*d*.

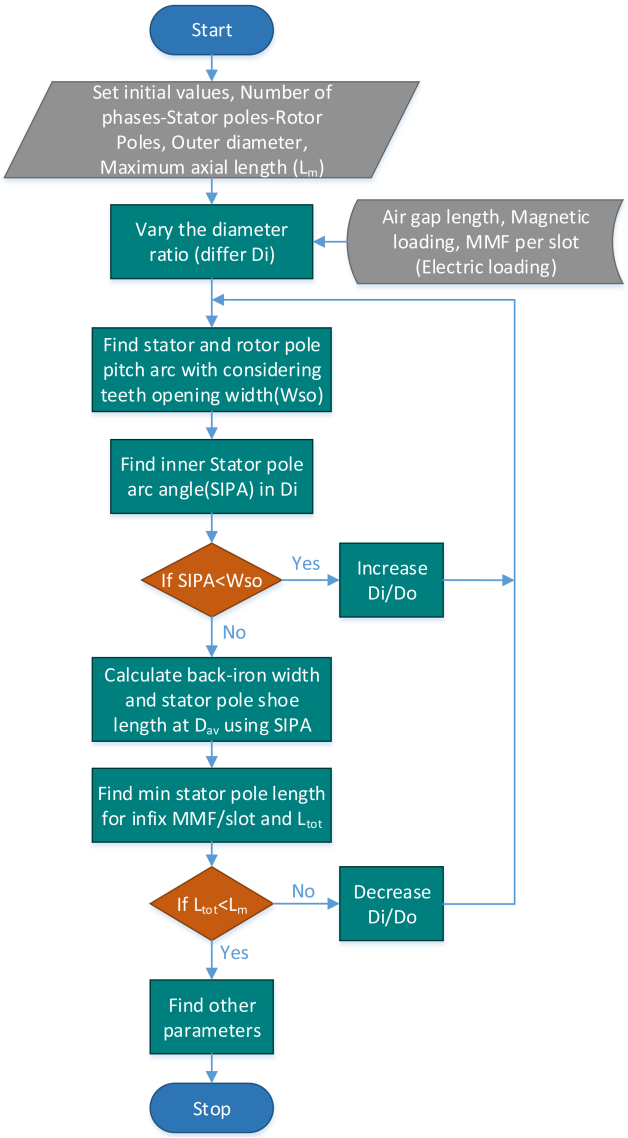

Fig. 3 *Flowchart of designing the segmented rotor AFSRM*

Another type of CS-AFSRM is seen in Fig. 15 which is modular and made up of some overlapping single phase CS-AFSRMs, and each layer shares specific magnetic features [82]. All layers are constructed similarly, but when assembling, the rotors are installed in a mechanical angle difference of one pole pitch divided by the number of phases, to one another. The stator which is salient consists of a circular coil and embraced by a toroidal C-shape core. Each tooth of the stator is considered to act like a pole. The rotor is segmented such that the tube segments are inserted inside a carrier disk, and all rotors' parts are coupled through a non-magnetic shaft to avoid forming any undesired magnetic paths. The suggested model in the reference is a six-layer six-phase machine which is made up of two three-phase units supplied by two common three-phase inverters [82]. The main problem of C-shape core machines is the high number of phases which increases the supplying system costs.

The inner heat is a limiting factor that affects the power density in electrical machines. AFSRMs are of the magnet-less structures. Therefore, a precise study on the thermal limitations of this machine will help to establish the determinants of performance indices such as current density. In SRMs, the hotspot point is generally located in the motor coils. But due to the higher core losses in the high frequency for high-speed structures, the temperature of these parts may be higher than others. For instance, a thermal analysis was performed for the CS-AFSRM in [38], the results of which can be seen in Fig. 16. According to the results, the temperature of the coils is the limiting factor for the power density. Thus, it is necessary to re-design the structure so that the temperature of the coils becomes lower than the thermal limit of copper wire.

4.2.3 IR-AFSRM: Interior rotor AFSRM (IR-AFSRM) only exists in segmented rotor type (IRS-AFSRM) [36, 37, 41, 75, 92, 104, 115] which is illustrated in Fig. 17. In this topology, the rotor is sandwiched by two quite similar stators, and number of stator poles exceeds the number of rotor poles. The stator consists of a steel lamination rolled like a toroid on which the slot positions are extracted, and a concentric winding surrounds the teeth.

The rotor is also segmented type, and the poles are inserted inside a non-magnetic carrier. It is recommended that the rotor poles are designed such that they form two flat surfaces on either side after installation in retainer disk. This causes the rotor poles not to act like a blade, and they also generate less noise [36, 75]; however, this is not considered in [37, 115]. Generally, the absence of yokes in the rotor improves axial length of the machines. According to Fig. 18, the main advantage of IRS-AFSRM versus SS-AFSRM is the magnetic force neutralisations regarding the stators symmetry. However, having two stators means that there are

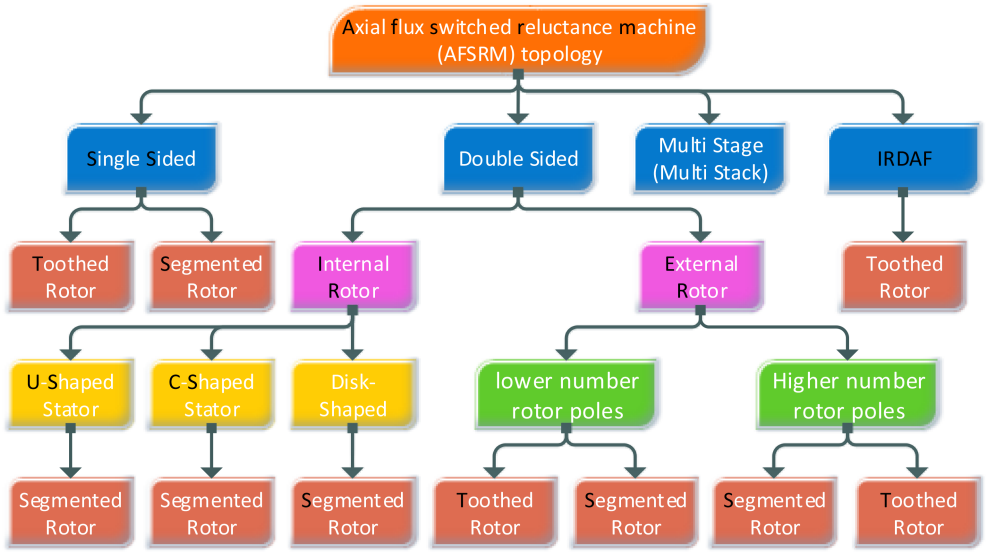

Fig. 4 *Assorted AFSRM topology classification*

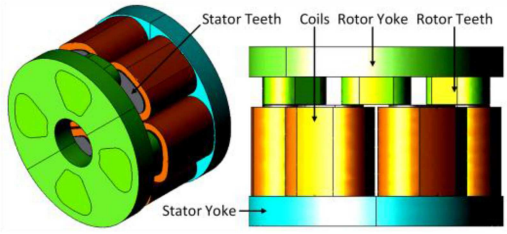

Fig. 5 *Three-dimensional structure of the SST-AFSRM*

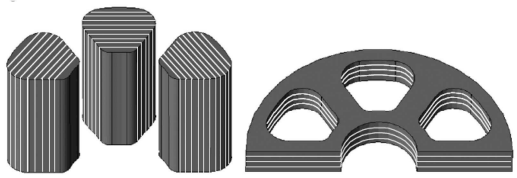

Fig. 6 *Lamination of stator's yoke and poles in SST-AFSSRM [29]*

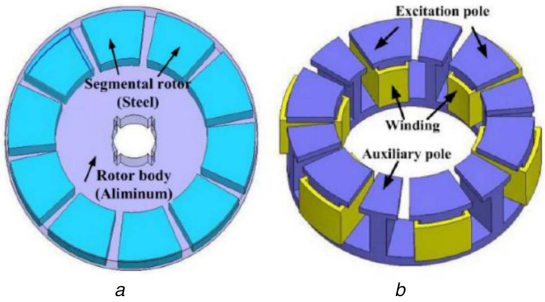

Fig. 7 *Structure of the SSS-AFSRM*
(a) Segmented rotor, ***(b)*** Stator and the windings [94]

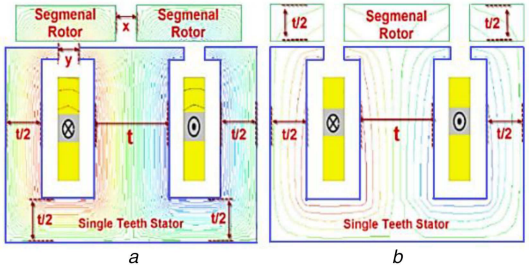

Fig. 8 *SSS-AFSRM flux path*
(a) Unaligned rotor position, ***(b)*** Aligned rotor position [103]

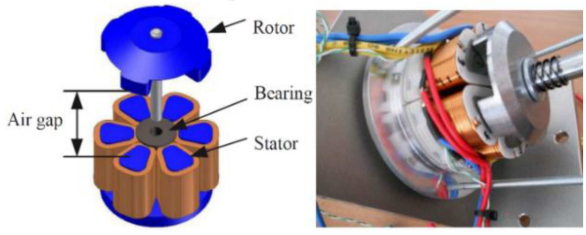

Fig. 9 *Constructed SST-AFSRM from magnetic composite [88]*

two air-gaps and maximum inductance is reduced, and consequently, power density is reduced [30].

4.2.4 ER-AFSRM: Exterior/external rotor AFSRM (ER-AFSRM) has been introduced as segmented and toothed pole topologies in two types of rotor pole numbers; higher and less than stator poles. The first machine with the aforementioned topology was initially designed for electric vehicle applications as a substitution for permanent magnet machines [116]. The author claims to have become closer to performance of the permanent magnet machines. This three-phase external rotor segmented AFSRM (ERS-AFSRM) with poles ratio of 12 to 8 and toroidal winding has been designed such that it produces higher torque compared to the radial flux salient SRMs.

The stator which is similar to a thick washer is designed in a way that the poles are put on either sides symmetrically. The circular concentric windings embrace the yoke, unlike the conventional AFSRMs which used to be wound on the teeth.

This has further shortened the flux path and reduced length of the end windings, and therefore, the iron and copper losses are reduced which subsequently leads to higher power density. Another advantage of this topology is that the axial forces applied on the stator have no effect on the windings and the results of the forces interact only with the rotor and the stator poles. In this topology, the coils of each phase can be connected in series or in parallel. The rotors are made in segments in a way that the poles are inserted inside an aluminium frame, and they are both installed on a shaft. This will increase the mechanical strength which is desired in high-speed operations and reduces the noise and the vibrations of the motor to a great extent. In addition, the stator is protected by two rotors and by connecting the rotors within the machines' outer diameter, the situation would be suitable for insertion inside the electric vehicle's wheel rim. However, the greater advantage is that the rotors act like a fan and the electrical loading can be increased [116]. In the two-rotor topology, the forces cause the rotors to be attracted to one another and hence a destructive force is applied on a part of the shaft which connects the two disks of the rotors. The topology and the magnetic flux paths in two positions of aligned and unaligned positions of the stator and the rotor poles in 2D and 3D view are illustrated in Figs. 19–21, respectively. In Fig. 22, an ERS-AFSRM is illustrated whose stator and rotor have 12 and 16 parts, respectively. This machine operates in three phases. In each phase, four coils are connected in series. The stator yoke is wound by the coils.

A hollow shaft is connected to the stator through which the machine's terminals are passed. Two rotor disks are connected externally, and they are directly connected to the considered electric vehicle wheels. The flux path in this topology is similar to Fig. 20, and the only structural difference is in the stator to rotor ratio.

AFSRM with external rotor can be of toothed pole type (ERT-AFSRM) [42, 117]. In this structure, there are two types introduced like ERS-AFSRM. Higher numbers (12/16) and less numbers (18/12) of rotor poles versus stator poles. As it is seen in Fig. 23, the stator is constructed as separate poles which are wound separately and held by a holder. In the absence of this holder disk, the poles cannot be tightened and fixed on their seat [40]. In this design, the coils may rob the stator teeth, the slots are considered thinner, and therefore, the aligned position reluctance is higher than the one of the segmented rotor type. For these machines, the maximum inductance is lower. This may be the result of a reduction factor of the torque. The salient type of rotor does not need the stator yoke. The flux is directed inside the stator by only a thin holder disk of a non-magnetic material. When slot space gets bigger, and MMF/slot is increased, the torque does not display a substantial difference as compared to the segmented rotor type. The flux path of ERT-AFSRM is illustrated in Fig. 24. The flux negotiates the axial length of the stator tooth and similarly closes its path by passing through two air-gaps, the teeth and another rotor's yoke.

4.3 MS-AFSRM

A multi-layer/multi-stack AFSRM (MS-AFSRM) can be constructed through SS- and DS-SRM structures which have already been explained. The multi-layer structure of AFSRM is created by at least three rotors or stators which are all installed on a shaft. In this type, the number of stators versus number of rotors can be equal, lower or higher. Ideally, the magnetic forces are well distributed in a situation in which there are N numbers of stators or rotors and $N \pm 1$ numbers of rotors or stators in which N represents the number of layers. The multi-layer topology can increase power and torque density for a constant outside diameter. This is because by increasing the number of rotors and stators, the ratio of air-gap numbers in proportion to stator and rotor numbers gets increased.

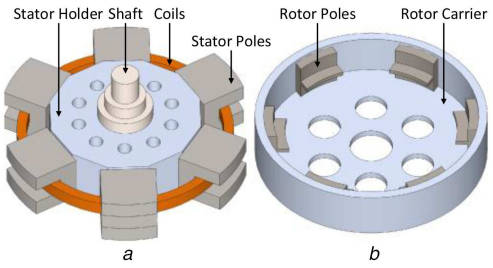

Fig. 10 *Single-phase US-AFSRM*
(a) Stator with winding, ***(b)*** Rotor and frame

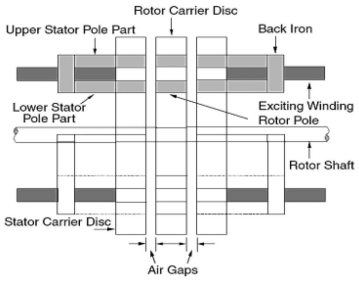

Fig. 11 *Three-phase US-AFSRM [5]*

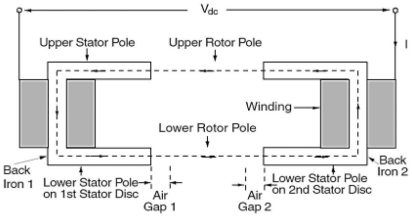

Fig. 12 *Magnetic flux path of the three-phase common US-AFSRM [5]*

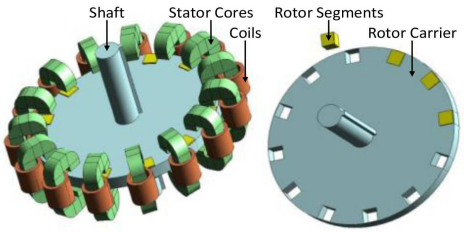

Fig. 13 *Typical CS-AFSRM*
(a) Motor without housing, ***(b)*** Rotor [105]

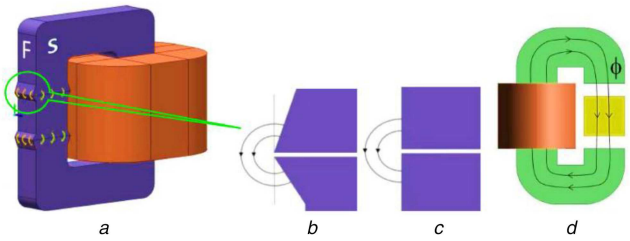

Fig. 14 *Poles in CS-AFSRM*
(a) 3D model, ***(b)*** Modified edge and flux longer path, ***(c)*** Original view of the pole, ***(d)*** Flux path [77, 105]

In other words, in ERT-AFSRM, there are two air-gaps despite having three rotor and stator pieces, but in MS-AFSRM for $N = 3$ there are four air-gaps per five pieces or six air-gaps per seven pieces of stator and rotor. In this design, the overall air-gap surfaces divided by the number (volume) of the utilised stators and rotors has been increased. The coil windings among the stators can be applied in series and in parallel. Compared with the MS-RFSRM, MS-AFSRM is simpler in construction since the air-gaps are flat and adjustable. MS-AFSRMs are available in salient and segmented rotors or a combination of them, with stator pole windings around the teeth or yokes. The magnetic flux path is

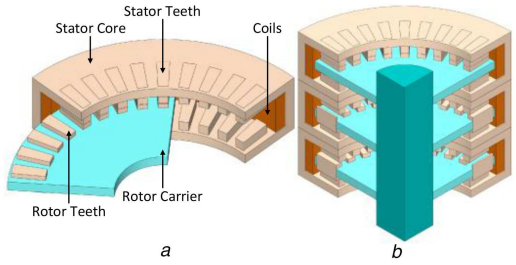

Fig. 15 *Modular CS-AFSRM*
(a) Cross-section of a single-phase CS-AFSRM, ***(b)*** Cross-section of a C-shape core three-phase machine

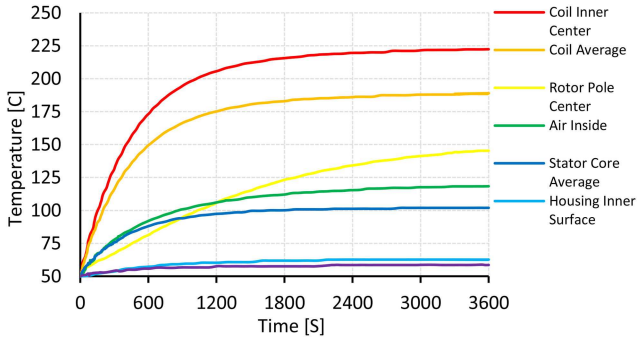

Fig. 16 *Temperature of different CS-AFSRM parts in 50°C of ambient temperature versus time [38]*

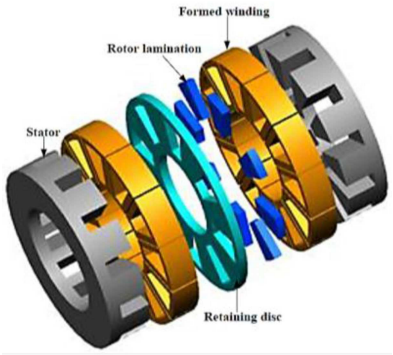

Fig. 17 *IRS-AFSRM [36]*

different according to the utilised basic topology. However, it is similar to the basic utilised structure, i.e. it can flow between the external two rotors (the middle rotors are independent of the yokes) or inside the body of all stators and rotors (each stator makes up a flux path with its two adjacent rotors). The advantages and disadvantages of the general structure are a complex of the structure's basic features employed in construction of the MS-AFSRM. The MS-AFSRM machines are longer in length. Therefore, the surface of the machine's frame is wider, and the generated heat is transferred easier.

4.4 IRD-AFSRM

One of the limiting factors of the torque density in AFSRM is the rotor's iron core saturation. Increase in the torque density can be accomplished by increasing volume of machine and the rotor and air-gaps. In [13], a combined topology which contains both types of axial flux and radial flux rotors namely as integrated radial and double AFSRM (IRD-AFSRM) has been analysed and compared with the conventional topologies which can be regarded as the improved topology of AFSRM through adding a rotor with the radial flux direction inside. The surrounding space of the stator is well employed, and length of the end winding has been decreased. This topology has 68% higher torque density compared to the conventional single rotor topologies.

Construction of a three-rotor machine has the advantage of higher winding coefficient in addition to lower magnetic saturation.

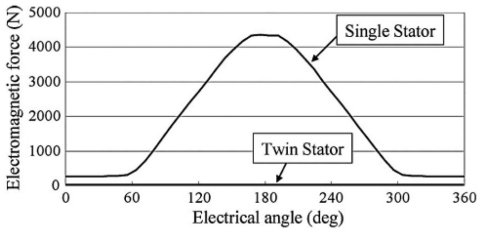

Fig. 18 *Comparison of the electromagnetic force between the rotor and the stator in single and double stator structures [30]*

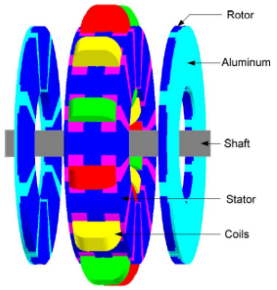

Fig. 19 *ERS-AFSRM with poles ratio of 12/8 [116]*

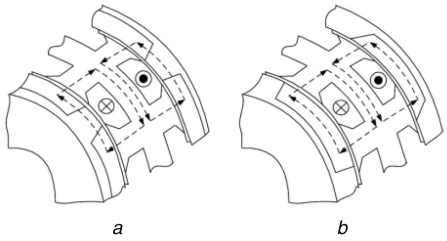

Fig. 20 *3D flux path in ERS-AFSRM*
(a) Unaligned, ***(b)*** Aligned [116]

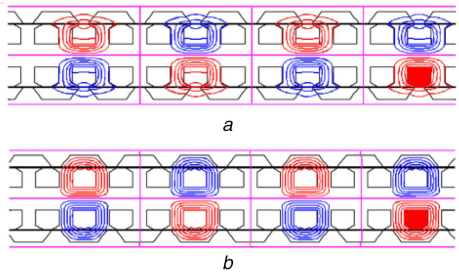

Fig. 21 *Linearised 2D flux path in ERS-AFSRM*
(a) Unaligned, ***(b)*** Aligned [116]

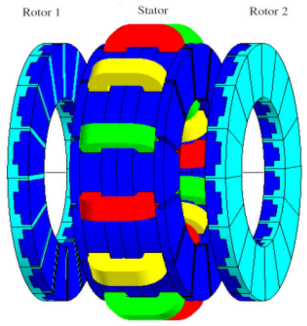

Fig. 22 *ERS-AFSSRM with higher number of the rotor poles versus the stator poles (12/16) [42]*

Compared to two-rotor AFSRM, the air-gap has become wider. Obviously, by increasing volume of rotors' cores and the air-gap surfaces, the machine needs to be redesigned so that the stator yoke calculations are done to avoid magnetic saturation in yokes, and the number of armature poles gets corrected. According to the results, the latter calculation shows 28% increase in the torque density [13]. As it is depicted in Fig. 25, the toroidal winding surrounds stator yoke, stator teeth face and teeth of three rotors. In this design, the stator and the rotor are both salient.

The majority of the parameters including volume and slot space are fixed, if the three RFSRM, ERT-AFSRM and IRD-AFSRM machines are compared. It is observed that the IRD-AFSRM torque is almost 2.2 times larger than torque of conventional radial flux SRM [13]. The torque–current characteristic of these three machines is shown in Fig. 26. Although the axial rotor disk machines have higher copper losses, according to Fig. 26, it is expected that efficiency of the IRD-AFSRM is increased. The complicated topology of three-rotor machines in which the magnetic flux flows in axial and radial directions, these machines need complicated process of laminating stator and rotor in different directions. To prevent the huge costs and to decrease the construction time, core is constructed with SMC in these machines. In the following, the aforementioned machines are compared structurally.

5 Performance indices evaluation and comparative study

As mentioned in introduction, different topologies of AFSRMs have never been compared comprehensively. Therefore, it is necessary to perform a functional comparison among various topologies which have already been presented. This could be regarded as a reference for researchers and engineers. For a fair comparison, equal situations are mandatory. Despite the comparable indices, some other indices as value per weight or volume density are compared so as to have comparable topologies which are of different weight and volume. Some examples include the average torque per weight or the output power per volume.

Since majority of sources do not mention the machines' weight and volume, these parameters are calculated based on the structural dimensions. However, some parameters cannot exactly be calculated, and sensitivity analyses are needed. It is impossible to choose the superior topology without sensitivity analysis. However, based on the desired function and the required characteristics a topology can be identified. In one case, the torque ripple may be of importance while in another case, efficiency or power density must be considered.

Fig. 27 depicts the efficiency of AFSRM of a number of designs from 77 to 90%. This type of machine is highly efficient, and the main reason would be the absence of rotor's (excitation) coil. However, the short path of magnetic flux in axial flux machines, especially in the segmented rotor type, has made their efficiency more than before since shortening of flux path results in lower loss of the magnetic cores. Results demonstrate that the external rotor topologies have better performance compared to other topologies which is due to motor advantages such as ease of installation and cooling, minimised mutual inductance with respect to self-inductance.

According to Fig. 28, range of the torque ripple takes up about <19–80% which proves that ripple torque entirely depends on structure. In SS- and US-AFSRM topologies, the torque ripple is higher and almost about 50–80% because the electromagnetic force has not been well distributed. In DS-SRM topologies, the torque ripple can be variable based on the selected structure. The segmented rotor topologies exhibit less torque ripple as compared to the salient pole topologies. The torque ripple increment may cause some troubles. As an example, in [77] when number of phases has increased results in decreasing the torque ripple. Increasing number of phases from the common case of 3 to 5, increases control and the drive prices. However, it decreases the ripple. Also, relative mechanical movement of rotors on the shaft and the rotor's side parts is utilised as a technique. In this case, the ripple has decreased as much as 38%. However, the possibility of the minus torque exists which decreases the average torque for as much as 3%. Furthermore, skewing the stator poles is utilised to decrease the torque ripple and has managed to decrease the torque ripple for as much as 18.5%. However, the average torque has decreased as 5.5% which is considerable. In [94], SSS-AFSRM has been proposed without any proposed solution to decrease the

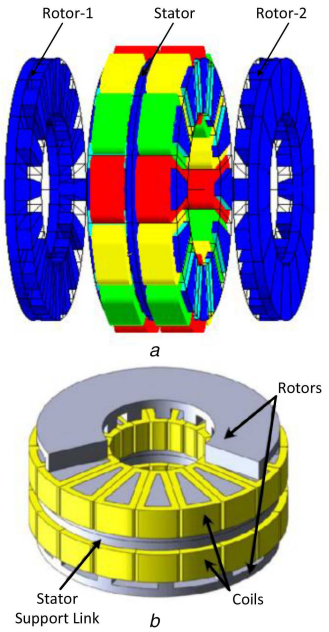

Fig. 23 *ERT-AFSRM with poles ratio of* ***(a)*** 12/16 [42], ***(b)*** 18/12 [40]

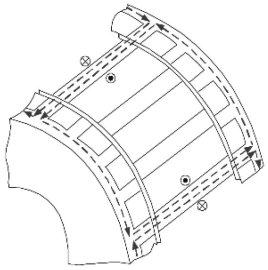

Fig. 24 *Magnetic flux path in ERT-AFSRM [42]*

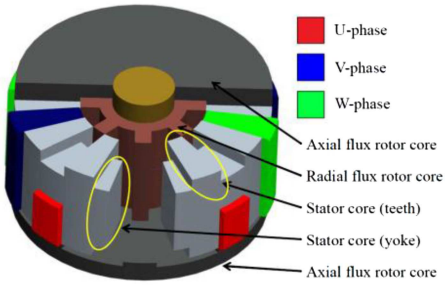

Fig. 25 *Three-dimensional view of IRD-AFSRM [13]*

torque ripple. This is why this topology has a high torque ripple value. It is not required to say that increasing the torque ripple helps generating the noise, but it is not its only reason. The unbalanced axial force is one of main reasons of vibration and acoustic noise generation which is tabulated in Table 1. The main problem of the torque ripple is the machine's vibration which makes the machine age and results in failure. Physical structure of the dynamic parts and their aerodynamic state is another reason of noise pollution. If the rotor is manufactured in an entirely cylinder smooth shape, there would not be high- and low-pressure points which ends up reducing noise. This can be implemented in segmented rotor topologies. A relative comparison between torque and power as functions of weight and volume densities lead to a fresh perspective on evaluation of each topology's capability. In this regard, in Table 1 some studied references are compared and evaluated.

The table depicts the highest torque density belongs to IRS-AFSRM topology which is around 4 N.m/kg. The reason is low weight of the rotor which is made of aluminium, and the magnetic parts of the rotor are too small. However, the highest power density

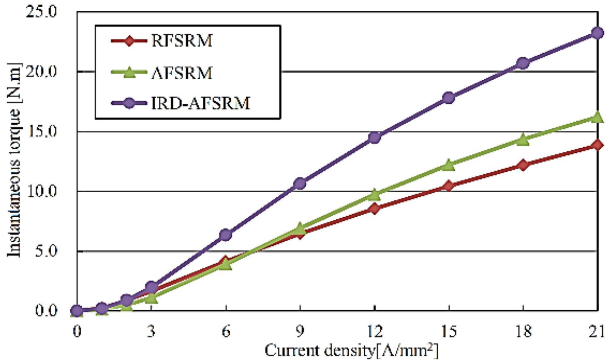

Fig. 26 *Torque density versus the current density [13]*

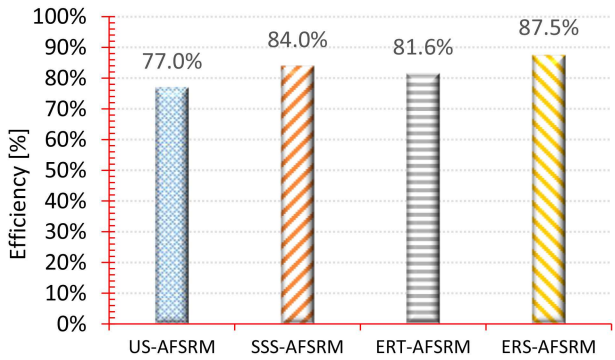

Fig. 27 *Comparing efficiency of different AFSRM types*

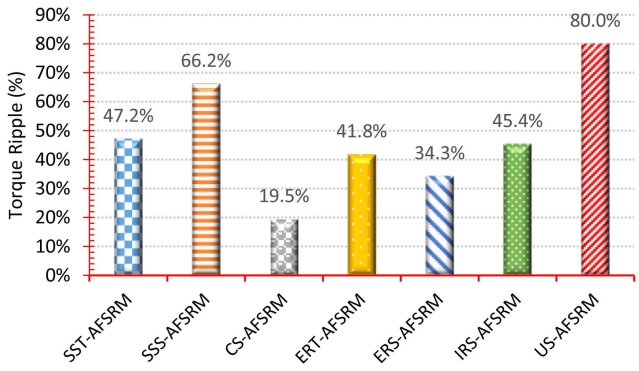

Fig. 28 *Torque ripple comparison of different types of AFSRMs*

is allocated to CS-AFSRM topology which is almost 4000 W/L, approximately two times larger than the average power density.

In an accurate investigation, one could conclude that the presented topologies in [35, 42] have acceptable torque density but rather undesirable power density. Despite producing desired torque in low weight, these topologies take up large spaces. The presented topology in [29], SST-AFSRM, has the comparable torque–power density with other topologies. However, this type has extremely high noise pollution and torque ripple that is why the general operation of this topology is questioned. Also, laminated structure of stator and rotor poles has various directions which increases the leakage flux and hence increases the loss.

The first presented AFSRM topology which possesses the U-shape structure of the stator [83] has the most minor operation since the number of the rotor and the stator poles are low and that there are three large disks to hold the magnetic cores of stator and rotor which increases weight and size of the machine. SSS-AFSRM has a rather more desired power density compared to torque density, and the reason is single-side SRM structure of the machine. This problem can be solved through designing the DS-SRM.

Table 1 Comparison of the operational characteristics in different types of AFSRM

Machine type		Pole ratio	Rated speed, rpm	Average torque, N.m	Output power, W	Active weight, kg	Active volume, m^3	Torque / weight, N.m/kg	Power / volume, W/m^3	Implementation	Cost	Axial forces	Vibration noise
US-AFSRM	[83]	3/2	1500	4.75	746	9.728	1.97	0.49	378.7	difficult	low	unbalanced	medium
SST-AFSRM	[29]	6/4	10,000	16.9	2750	8.23	1.547	2.05	1777	easy	medium	unbalanced	high
CS-AFSRM	[77]	15/12	2400	37	9000	16.7	2.165	2.21	4157	difficult	low	balanced	low
ERT-AFSRM	[42]	12/16	600	20.75	1300	11.2	1.47	1.85	880	moderate	high	balanced	medium
ERS-AFSRM	[35]	12/16	600	24.12	1515	13.2	1.88	1.83	805	difficult	high	balanced	medium
SSS-AFSRM	[80]	12/10	2800	1.97	577	1.66	0.24	1.19	2400	moderate	medium	unbalanced	high
IRS-AFSRM	[36]	12/8	650	68.7	4670	17.02	2.24	4.03	2084	difficult	medium	balanced	low

6 Conclusion

In this paper, a comprehensive review was undertaken on the assorted types of AFSRMs which have already been presented. AFSRMs were introduced, and their advantages and disadvantages were discussed. Also, their applications, investigation necessity, design considerations, limitations and operation characteristics were investigated. The detailed classification of all topologies of AFSRMs was suggested. The topologies were first classified according to the physical forms and number of the air-gap surfaces, and then, structural differences and features were widely discussed based on operation principles and advantages and disadvantages. The electromagnetic force analysis and its influence on the machines' vibrations were investigated in assorted topologies. In the final section, a comprehensive comparison was made on the operational characteristics of all topologies. The AFSRM torque ripple is between 19 and 80 and entirely depends on structure type whereas efficiency of these machines is in a fixed range with an average of 80. The power and torque densities are, respectively, in the range of 0.5–4 and 400–4000. In this paper, an operational policy is designed for the AFSRM designers governing further developments of this topology.

In order to create a novel framework, we can point out: investigating multi-stack structures can help improve the AFSRM power density. Using SMC to build the core of these machines can be considered as a good potential, which reduces the cost of construction and implementation difficulties and increases the ability to deal with noise. Also, providing the non-magnetic structure is a good challenge for the producers, nowadays. In addition, modern structures may improve the quality of power and the torque density of these structures, despite multiple air-gap radial, axial or transversal directions.

7 Acknowledgments

This work was supported by research grants from the Niroo Research Institute (NRI), Tehran, Iran.

8 References

[1] Jiang, J.W., Bilgin, B., Emadi, A.: 'Three-phase 24/16 switched reluctance machine for a hybrid electric powertrain', *IEEE Trans. Transp. Electrification*, 2017, **3**, (1), pp. 76–85

[2] Bostanci, E., Moallem, M., Parsapour, A., *et al.*: 'Opportunities and challenges of switched reluctance motor drives for electric propulsion: a comparative study', *IEEE Trans. Transp. Electrification*, 2017, **3**, (1), pp. 58–75

[3] Lin, J., Schofield, N., Emadi, A.: 'External-rotor switched reluctance motor for an electric bicycle', *IEEE Trans. Transp. Electrification*, 2015, **1**, (4), pp. 348–356

[4] Miller, T.J.E.: '*Switched reluctance motor drives: a reference book of collected papers*' (Intertec Communications, Incorporated, U.K., 1988)

[5] Krishnan, R.: '*Switched reluctance motor drives: modeling, simulation, analysis, design, and applications*' (CRC Press, USA., 2001)

[6] Torkaman, H., Faraji, N., Toulabi, M.S.: 'Influence of rotor structure on fault diagnosis indices in two-phase switched reluctance motors', *IEEE Trans. Magn.*, 2014, **50**, (3), pp. 136–143

[7] Asgar, M., Afjei, E., Torkaman, H.: 'A new strategy for design and analysis of a double-stator switched reluctance motor: electromagnetics, FEM, and experiment', *IEEE Trans. Magn.*, 2015, **51**, (12), pp. 1–8

[8] Torkaman, H., Afjei, E.: 'Sensorless method for eccentricity fault monitoring and diagnosis in switched reluctance machines based on stator voltage signature', *IEEE Trans. Magn.*, 2013, **49**, (2), pp. 912–920

[9] Afjei, E., Siadatan, A., Torkaman, H.: 'Magnetic modeling, prototyping, and comparative study of a quintuple-set switched reluctance motor', *IEEE Trans. Magn.*, 2015, **51**, (8), pp. 1–7

[10] Nezamabadi, M.M., Afjei, E., Torkaman, H.: 'Design, dynamic electromagnetic analysis, FEM, and fabrication of a new switched-reluctance motor with hybrid motion', *IEEE Trans. Magn.*, 2016, **52**, (4), pp. 1–8

[11] Castano, S.M., Bilgin, B., Fairall, E., *et al.*: 'Acoustic noise analysis of a high-speed high-power switched reluctance machine: frame effects', *IEEE Trans. Energy Convers.*, 2016, **31**, (1), pp. 69–77

[12] Zhou, H., Cao, X., Qiao, Y., *et al.*: 'A novel 6/4 conical bearingless switched reluctance motor'. 18th Int. Conf. on Electrical Machines and Systems (ICEMS), Pattaya, 2015

[13] Fukai, D., Shimomura, S.: 'Integrated radial and dual axial-flux variable-reluctance vernier machine'. 40th Annual Conf. of the IEEE Industrial Electronics Society, Dallas, TX, 2014, pp. 682–688

[14] Jianfei, P., Fanjie, M., Guangzhong, C.: 'Decoupled control for integrated rotary linear switched reluctance motor', *Electr. Power Appl.*, 2014, **8**, (5), pp. 199–208

[15] Bilgin, B., Emadi, A., Krishnamurthy, M.: 'Comprehensive evaluation of the dynamic performance of a 6/10 SRM for traction application in PHEVs', *IEEE Trans. Ind. Electron.*, 2013, **60**, (7), pp. 2564–2575

[16] Hua, W., Hua, H., Xu, X., *et al.*: 'Analysis and experimental validation of a half-teeth-wound switched reluctance machine', *IEEE Trans. Magn.*, 2014, **50**, (11), pp. 1–5

[17] Kabir, M.A., Husain, I.: 'Design of mutually coupled switched reluctance motors (MCSRMs) for extended speed applications using 3-phase standard inverters', *IEEE Trans. Energy Convers.*, 2016, **31**, (2), pp. 436–445

[18] Lin, C., Wang, W., McDonough, M., *et al.*: 'An extended field reconstruction method for modeling of switched reluctance machines', *IEEE Trans. Magn.*, 2012, **48**, (2), pp. 1051–1054

[19] Ding, W., Liu, L., Lou, J.: 'Design and control of a high-speed switched reluctance machine with conical magnetic bearings for aircraft application', *IET Electr. Power Appl.*, 2013, **7**, (3), pp. 179–190

[20] Wang, D., Wang, X., Du, X.F.: 'Design and comparison of a high force density dual-side linear switched reluctance motor for long rail propulsion application with low cost', *IEEE Trans. Magn.*, 2017, **53**, (6), pp. 1–4

[21] Du, J., Liang, D., Liu, X.: 'Performance analysis of a mutually coupled linear switched reluctance machine for direct-drive wave energy conversions', *IEEE Trans. Magn.*, 2017, **53**, (9), pp. 1–10

[22] Chen, H., Nie, R., Sun, M., *et al.*: '3-D electromagnetic analysis of single-phase tubular switched reluctance linear launcher', *IEEE Trans. Plasma Sci.*, 2017, **45**, (7), pp. 1553–1560

[23] Pan, J.F., Yu, Z., Cheung, N.C.: 'Performance analysis and decoupling control of an integrated rotary linear machine with coupled magnetic paths', *IEEE Trans. Magn.*, 2014, **50**, (2), pp. 761–764

[24] Benția, I., Ruba, M., Szabó, L.: 'On the control of a rotary-linear switched reluctance motor'. 5th Int. Symp. on Computational Intelligence and Intelligent Informatics (ISCIII), Floriana, 2011, pp. 41–46

[25] Safdarzadeh, O., Afjei, E., Torkaman, H.: 'Effective magnetic decoupling control realization for rotary-linear switched reluctance motors utilized in drilling tools', *Int. J. Appl. Electromagn. Mech.*, 2018, **57**, (3), pp. 257–274

[26] Locment, F., Semail, E., Piriou, F.: 'Design and study of a multiphase axial-flux machine', *IEEE Trans. Magn.*, 2006, **42**, (4), pp. 1427–1430

[27] Vansompel, H., Sergeant, P., Dupre, L., *et al.*: 'Evaluation of a simple lamination stacking method for the teeth of an axial flux permanent-magnet

synchronous machine with concentrated stator windings', *IEEE Trans. Magn.*, 2012, **48**, (2), pp. 999–1002
[28] Deguchi, K., Sumita, S., Enomoto, Y.: 'A 3.7-kW axial-gap switched-reluctance motor robustly designed by using a mathematical model'. Int. Conf. on Electrical Machines (ICEM), Berlin, 2014, pp. 340–345
[29] Arihara, H., Akatsu, K.: 'Characteristics of axial type switched reluctance motor'. IEEE Energy Conversion Congress and Exposition (ECCE), Phoenix, AZ, 2011, pp. 3582–3589
[30] Arihara, H., Akatsu, K.: 'Basic properties of an axial-type switched reluctance motor', *IEEE Trans. Ind. Electron.*, 2013, **49**, (1), pp. 59–65
[31] Ma, J., Li, J., Fang, H., *et al.*: 'Optimal design of an axial-flux switched reluctance motor with grain-oriented electrical steel', *IEEE Trans. Ind. Appl.*, 2017, **53**, (6), pp. 5327–5337
[32] Madhavan, R., Fernandes, B.G.: 'Performance improvement in the axial flux-segmented rotor-switched reluctance motor', *IEEE Trans. Energy Convers.*, 2014, **29**, (3), pp. 641–651
[33] Labak, A., Kar, N.C.: 'Development and analysis of a five-phase pancake shaped switched reluctance motor'. 2010 XIX Int. Conf. on Electrical Machines (ICEM), Rome, 2010, pp. 1–6
[34] Ega, I., Argando, I.R.d., Madariaga, J.: 'Analytical electromagnetic model of modular axialflux switched-reluctance machine'. Eleventh Int. Conf. on Ecological Vehicles and Renewable Energies, Monte Carlo, 6–8 April 2016
[35] Madhavan, R., Fernandes, B.G.: 'Axial flux segmented SRM with a higher number of rotor segments for electric vehicles', *IEEE Trans. Energy Convers.*, 2013, **28**, (1), pp. 203–213
[36] Jimin, M., Ronghai, Q., Jian, L.: 'Optimal design of axial flux switched reluctance motor for electric vehicle application'. 17th Int. Conf. on Electrical Machines and Systems (ICEMS), Hangzhou, 2014, pp. 1860–1865
[37] Sengupta, M., Ahmad, S.S., Mukherjee, D.: 'Experimental investigations on a novel laboratory prototype of axial flux switched reluctance motor'. IEEE Int. Conf. on Power Electronics, Drives and Energy Systems (PEDES), Bengaluru, 2012, pp. 1–5
[38] Chong, Y.C., Staton, D., Egaña, I., *et al.*: 'Thermal design of a magnet-free axial-flux switch reluctance motor for automotive applications'. Eleventh Int. Conf. on Ecological Vehicles and Renewable Energies (EVER), Monte Carlo, 2016, pp. 1–8
[39] Potgieter, J.H.J., Márquez-Fernández, F.J., Fraser, A.G., *et al.*: 'Performance evaluation of a high speed segmented rotor axial flux switched reluctance traction motor'. XXII Int. Conf. on Electrical Machines (ICEM), Lausanne, 2016, pp. 531–537
[40] Goto, H., Shibamoto, T., Nakamura, K., *et al.*: 'Development of high torque density axial-gap switched reluctance motor for in-wheel direct-drive EV'. 15th European Conf. on Power Electronics and Applications (EPE), Lille, 2013, pp. 1–7
[41] Goto, H., Murakami, S., Ichinokura, O.: 'Design to maximize torque-volume density of axial-flux SRM for in-wheel EV'. 41st Annual Conf. of the IEEE Industrial Electronics Society, Yokohama, 2015, pp. 005191–005196
[42] Madhavan, R., Fernandes, B.G.: 'Comparative analysis of axial flux SRM topologies for electric vehicle application'. IEEE Int. Conf. on Power Electronics, Drives and Energy Systems (PEDES), Bengaluru, 2012, pp. 1–6
[43] Krebs, G., de Cecco, E., Marchand, C.: 'Design approach of an axial flux motor for electrical powertrain vehicle'. XXth Int. Conf. on Electrical Machines (ICEM), Marseille, 2012, pp. 2812–2817
[44] Tsai, J.-F., Chen, Y.-P.: 'Design and performance analysis of an axial-flux disk-type switched reluctance motor for hybrid scooters', *JSME Int. J. C*, 2006, **49**, (3), p. 8
[45] Andrada, P., Martínez, E., Blanqué, B., *et al.*: 'New axial-flux switched reluctance motor for E-scooter'. Int. Conf. on Electrical Systems for Aircraft, Railway, Ship Propulsion and Road Vehicles & Int. Transportation Electrification Conf., Toulouse, 2016, pp. 1–6
[46] Cheng-Tsung, L., Yen-Ming, C., Da-Chen, P.: 'Optimal design of a micro axial flux switched-reluctance motor'. IEEE Int. Conf. on Electric Machines and Drives, San Antonio, TX, 2005, pp. 1130–1134
[47] Cheng-Tsung, L., Yen-Ming, C., Da-Chen, P.: 'Performance index evaluations of a micro axial-flux switched-reluctance motor'. IEEE 5th Int. Power Electronics and Motion Control Conf., IPEMC, Shanghai, 14–16 August 2006
[48] de Castro Teixeira, V.S., Ruppert Filho, E., dos Santos Barros, T.A., *et al.*: 'Design, optimization and analysis of the axial C-core switched reluctance generator for wind power application'. Int. Conf. on Renewable Energy Research and Applications, Palermo, 2015, pp. 833–837
[49] Jun-Young, L., Hyung-Sup, K., Jae-Yoon, O., *et al.*: 'A performance of single phase switched reluctance motor having both radial and axial air gap'. 24th Annual Conf. of the IEEE Industrial Electronics Society, Aachen, Germany, 1998, vol. 2, pp. 905–910
[50] Yang, Z., Shang, F., Brown, I.P., *et al.*: 'Comparative study of interior permanent magnet, induction, and switched reluctance motor drives for EV and HEV applications', *IEEE Trans. Transp. Electrification*, 2015, **1**, (3), pp. 245–254
[51] Boldea, I., Tutelea, L.N., Parsa, L., *et al.*: 'Automotive electric propulsion systems with reduced or no permanent magnets: an overview', *IEEE Trans. Ind. Electron.*, 2014, **61**, (10), pp. 5696–5711
[52] Mojlish, S., Erdogan, N., Levine, D., *et al.*: 'Review of hardware platforms for real-time simulation of electric machines', *IEEE Trans. Transp. Electrification*, 2017, **3**, (1), pp. 130–146
[53] Daghigh, A., Javadi, H., Torkaman, H.: 'Design optimization of direct-coupled ironless axial flux permanent magnet synchronous wind generator with low cost and high annual energy yield', *IEEE Trans. Magn.*, 2016, **52**, (9), pp. 1–11
[54] Khaliq, S., Atiq, S., Lipo, T.A., *et al.*: 'Rotor pole optimization of novel axial-flux brushless doubly fed reluctance machine for torque enhancement', *IEEE Trans. Magn.*, 2016, **52**, (7), pp. 1–4
[55] Joseph, B.G., Thomas, P.: 'Variable reluctance axial flux alternator incorporating air gap variation'. Int. Conf. on Power and Energy Systems: Towards Sustainable Energy, Bangalore, 2016
[56] Fasil, M., Mijatovic, N., Jensen, B.B., *et al.*: 'Finite-element model-based design synthesis of axial flux PMBLDC motors', *IEEE Trans. Appl. Supercond.*, 2016, **26**, (4), pp. 1–5
[57] Daghigh, A., Javadi, H., Torkaman, H.: 'Improved design of coreless axial flux permanent magnet synchronous generator with low active material cost'. The 6th Power Electronics, Drive Systems & Technologies Conf., Iran, 2015, pp. 532–537
[58] Torkaman, H., Ghaheri, A., Keyhani, A.: 'Design of rotor excited axial flux-switching permanent magnet machine', *IEEE Trans. Energy Convers.*, 2018, **33**, (3), pp. 1175–1183
[59] Caricchi, F., Crescimbini, F., Honorati, O., *et al.*: 'Performance of coreless-winding axial-flux permanent-magnet generator with power output at 400 Hz, 3000 r/min', *IEEE Trans. Ind. Electron.*, 1998, **34**, (6), pp. 1263–1269
[60] Cavagnino, A., Lazzari, M., Profumo, F., *et al.*: 'Axial flux interior PM synchronous motor: parameters identification and steady-state performance measurements', *IEEE Trans. Ind. Electron.*, 2000, **36**, (6), pp. 1581–1588
[61] Wenliang, Z., Lipo, T.A., Byung-il, K.: 'Comparative study on novel dual stator radial flux and axial flux permanent magnet motors with ferrite magnets for traction application', *IEEE Trans. Magn.*, 2014, **50**, (11), pp. 1–4
[62] De Donato, G., Capponi, F.G., Rivellini, G.A., *et al.*: 'Integral-slot versus fractional-slot concentrated-winding axial-flux permanent-magnet machines: comparative design, FEA, and experimental tests', *IEEE Trans. Ind. Electron.*, 2012, **48**, (5), pp. 1487–1495
[63] Mahmoudi, A., Rahim, N., Hew, W.: 'Axial-flux permanent-magnet machine modeling, design, simulation, and analysis', *Sci. Res. Essays*, 2011, **6**, (12), pp. 2525–2549
[64] Bojoi, R., Pellegrino, G., Cavagnino, A., *et al.*: 'Direct flux vector control of axial flux IPM motors for in-wheel traction solutions'. 36th Annual Conf. on IEEE Industrial Electronics Society, Glendale, AZ, 2010, pp. 2224–2229
[65] Jurca, F., Fodorean, D.: 'Axial flux interior permanent magnet synchronous motor for small electric traction vehicle'. Int. Symp. on Power Electronics, Electrical Drives, Automation and Motion (SPEEDAM), Italy, 2012, pp. 365–368
[66] Aydin, M., Huang, S., Lipo, T.: 'Axial flux permanent magnet disc machines: a review'. Proc. of the SPEEDAM, Italy, 2004
[67] El-Refaie, A.M.: 'Fault-tolerant permanent magnet machines: a review', *Electr. Power Appl.*, 2011, **5**, (1), pp. 59–74
[68] Kahourzade, S., Mahmoudi, A., Hew Wooi, P., *et al.*: 'A comprehensive review of axial-flux permanent-magnet machines', *Can. J. Electr. Comput. Eng.*, 2014, **37**, (1), pp. 19–33
[69] Nasiri-Gheidari, Z., Lesani, H.: 'A survey on axial flux induction motors', *Prz. Elektrotech., Electr. Rev.*, 2012, **88**, (2), pp. 300–305
[70] Vijayakumar, K., Karthikeyan, R., Paramasivam, S., *et al.*: 'Switched reluctance motor modeling, design, simulation, and analysis: a comprehensive review', *IEEE Trans. Magn.*, 2008, **44**, (12), pp. 4605–4617
[71] Wei, X., Jianguo, Z., Youguang, G., *et al.*: 'Survey on electrical machines in electrical vehicles'. Int. Conf. on Applied Superconductivity and Electromagnetic Devices, Chengdu, 2009, pp. 167–170
[72] Gao, Y., McCulloch, M.D.: 'A review of high power density switched reluctance machines suitable for automotive applications'. XXth Int. Conf. on Electrical Machines (ICEM), Marseille, 2012, pp. 2610–2614
[73] Chiba, A., Kiyota, K.: 'Review of research and development of switched reluctance motor for hybrid electrical vehicle'. IEEE Workshop on Electrical Machines Design, Control and Diagnosis (WEMDCD), Torino, 2015, pp. 127–131
[74] Torkaman, H., Keyhani, A.: 'A review of design consideration for Doubly Fed Induction Generator based wind energy system', *Electr. Power Syst. Res.*, 2018, **160**, pp. 128–141
[75] Daldaban, F., Ustkoyuncu, N.: 'New disc type switched reluctance motor for high torque density', *Energy Convers. Manage.*, 2007, **48**, (8), pp. 2424–2431
[76] Goodier, E.R.T., Pollock, C.: 'Homopolar variable reluctance machine incorporating an axial field coil', *IEEE Trans. Ind. Electron.*, 2002, **38**, (6), pp. 1534–1541
[77] Labak, A., Kar, N.C.: 'Designing and prototyping a novel five-phase pancake-shaped axial-flux SRM for electric vehicle application through dynamic FEA incorporating flux-tube modeling', *IEEE Trans. Ind. Electron.*, 2013, **49**, (3), pp. 1276–1288
[78] Lee, C., Liu, C., Chau, K.: 'A magnetless axial-flux machine for range-extended electric vehicles', *Energies*, 2014, **7**, (3), p. 1483
[79] Egea, A., Ugalde, G., Poza, J., *et al.*: 'FEM model validation for modular axial flux switched reluctance machine design switched reluctance machine design'. Eleventh Int. Conf. on Ecological Vehicles and Renewable Energies (EVER), Monte Carlo, 2016, pp. 1–5
[80] Bo, W., Dong-Hee, L., Jin-Woo, A.: 'Segmental rotor axial field switched reluctance motor with single teeth winding'. IEEE 23rd Int. Symp. on Industrial Electronics (ISIE), Istanbul, 1–4 June 2014
[81] Bo, W., Dong-Hee, L., Jin-Woo, A.: 'Characteristic analysis of a novel segmental rotor axial field switched reluctance motor with single teeth winding'. IEEE Int. Conf. on Industrial Technology (ICIT), Busan, 26 February 2014–1 March 2014
[82] Bolognesi, P.: 'Design and manufacturing of an unconventional variable reluctance machine'. 4th IET Conf. on Power Electronics, Machines and Drives, York, 2008, pp. 45–49
[83] Krishnan, R., Abouzeid, M., Mang, X.: 'A design procedure for axial field switched reluctance motors'. IEEE Industry Applications Society Annual Meeting, Seattle, WA, USA, 1990, vol. 1, pp. 241–246
[84] Sanches, E.S., Santisteban, J.A.: 'Implementing a neural PID speed controller for a single stator axial flux switched reluctance motor aiming torque ripple

minimization'. Brazilian Power Electronics Conf. (COBEP), Brazil, 27–31 October 2013
[85] Ebrahimi, Y., Feyzi, M.: 'A high torque density axial flux SRM with modular stator', *Iran. J. Electr. Electron. Eng.*, 2015, **11**, (4), pp. 336–344
[86] Kordkandi, D.T., Gardeshi, H.K., Torkaman, H.: 'An improved method to control the speed and flux of PM-BLDC motors'. The 6th Power Electronics, Drive Systems & Technologies Conf. (PEDSTC2015), Tehran, Iran, 2015, pp. 639–644
[87] Mansouri, S., Allahverdinejad, B., Torkaman, H.: 'Power factor correction based hybrid resonance PWM fed BLDC drive'. 9th Annual Power Electronics, Drives Systems and Technologies Conf. (PEDSTC), Tehran, Iran, 2018, pp. 77–82
[88] Kellerer, T., Radler, O., Sattel, T., *et al.*: 'Axial type switched reluctance motor of soft magnetic composite'. Innovative Small Drives and Micro-Motor Systems, GMM/ETG Symp., Nuremberg, Germany, 2013, pp. 1–6
[89] Porzig, K., Ziolkowski, M., Brauer, H., *et al.*: 'Fast simulations of 3D axial switched reluctance motor drives'. COMPUMAG, Budapest, 2013
[90] Lambert, T., Biglarbegian, M., Mahmud, S.: 'A novel approach to the design of axial-flux switched-reluctance motors', *Machines*, 2015, **3**, (1), pp. 27–54
[91] Labak, A., Kar, N.C.: 'Novel approaches towards leakage flux reduction in axial flux switched reluctance machines', *IEEE Trans. Magn.*, 2013, **49**, (8), pp. 4738–4741
[92] Ma, J., Qu, R., Li, J.: 'A novel axial flux switched reluctance motor with grain oriented electrical steel'. IEEE Magnetics Conf. (INTERMAG), Beijing, 2015, pp. 1–1
[93] Ma, J., Qu, R., Li, J.: 'Optimal design of an axial flux switched reluctance motor with grain oriented electrical steel'. 18th Int. Conf. on Electrical Machines and Systems, Pattaya, 2015, pp. 2071–2077
[94] Wang, B., Jin-Woo, A.: 'Design and characteristic analysis of a novel axial field SRM with single teeth stator and segmental rotor'. Int. Conf. on Electrical Machines and Systems, Busan, 26–29 October 2013
[95] Lambert, T.: 'A novel approach to the design of an in-wheel semi-anhysteretic axial-flux switched-reluctance motor drive system for electric vehicles', 2013
[96] Nelson, A.L.: 'Characterization of winding faults in axial flux reluctance motors in the context of electric vehicle propulsion systems', 2000
[97] Labak, A.: 'New design of switched reluctance motor using finite element analysis for hybrid electric vehicle applications', 2010
[98] Itsuya, M., Nakamura, T., Hun-June, J., *et al.*: 'Starting and steady state characteristics of axial-type high T/sub c/ superconducting bulk motor'. Sixth Int. Conf. on Electrical Machines and Systems, Beijing, China, 2003, vol. 1, pp. 238–241
[99] Jong-Han, L., Eun-Woong, L., Chung-Won, L.: 'Analysis of the characteristics of the disk type single phase SRM'. Sixth Int. Conf. on Electrical Machines and Systems, Beijing, China, 2003, vol. 1, pp. 230–233
[100] Lambert, T., Biglarbegian, M., Mahmud, S.: 'Development of novel controllers for an axial-flux switched-reluctance motor', *J. Control Autom. Electr. Syst.*, 2014, **25**, (6), pp. 629–638
[101] Madhavan, R., Fernandes, B.G.: 'A novel technique for minimizing torque ripple in axial flux segmented rotor SRM'. IEEE Energy Conversion Congress and Exposition (ECCE), Phoenix, AZ, 17–22 September 2011
[102] Abou-Zaid, M., El-Attar, M., Moussa, M.: 'Analysis and performance of axial field switched reluctance generator'. Electric Machines and Drives, Int. Conf. IEMD, Seattle, WA, USA, 1999, pp. 141–143
[103] Wang, B., Dong-Hee, L., Jin-Woo, A.: 'A novel axial field SRM with segmental rotor: concept, design and analysis'. Workshop on Power Electronics and Power Quality Applications (PEPQA), Bogota, 2013, pp. 1–6
[104] Pulle, D.W.J., Petersen, I.R.: 'A unified approach to switched reluctance drive modeling: application to an axial flux (SRAF) motor'. 29th Annual IEEE Power Electronics Specialists Conf., Fukuoka, 1998, vol. 2, pp. 1681–1686
[105] Labak, A., Kar, N.C.: 'A novel five-phase pancake shaped switched reluctance motor for hybrid electric vehicles'. Vehicle Power and Propulsion Conf., Dearborn, MI, 2009, pp. 494–499
[106] Goodier, E.R.T., Pollock, C.: 'Homopolar variable reluctance machine incorporating an axial field coil'. IEEE Industry Applications Conf. Thirty-Sixth IAS Annual Meeting, Chicago, IL, USA, 2001, vol. 3, pp. 1997–2004
[107] Goodier, E.R.T.: 'Reluctance machines with flux assistance'. PhD, Engineering, University of Leicester, United Kingdom, 2003
[108] Egea, A., Ugalde, G., Poza, J.: 'Torque control strategy for an axial flux switched reluctance machine'. XXII Int. Conf. on Electrical Machines, Lausanne, 4–7 September 2016
[109] Arihara, H., Akatsu, K.: 'A basic property of axial type Switched Reluctance Motor'. Int. Conf. on Electrical Machines and Systems, Incheon, 2010, pp. 1687–1690
[110] Kyoung-Ho, K., Yun-Hyun, C., Do-Hyun, K., *et al.*: 'Characteristics analysis of axial flux type reluctance motor using 2 and 3-dimensional finite element method'. IEEE Int. Symp. on Industrial Electronics Proc., Pusan, South Korea, 2001, vol. 2, pp. 1169–1174
[111] Sanches, E.S., Santisteban, J.A.: 'Comparative study of conventional, fuzzy logic and neural PID speed controllers with torque ripple minimization for an axial magnetic flux switched reluctance motor', *Engineering*, 2014, **6**, (11), p. 655
[112] Krishnan, R., Beutler, A.: 'Performance and design of an axial field permanent magnet synchronous motor servo drive'. Proc. IEEE Industrial Applications Society Annual Meeting, Austin, 1985, pp. 634–640
[113] Krishnan, R., Arumugan, R., Lindsay, J.F.: 'Design procedure for switched-reluctance motors', *IEEE Trans. Ind. Appl.*, 1988, **24**, (3), pp. 456–461
[114] Sass, F., Santisteban, J.A., Sanches, E.: 'Design and implementation of a digital control system for an axial flux switched reluctance motor'. Brazilian Power Electronics Conf., Bonito-Mato Grosso do Sul, 2009, pp. 138–144
[115] Kermanipour, M.J., Ganji, B.: 'Modification in geometric structure of double-sided axial flux switched reluctance motor for mitigating torque ripple', *Can. J. Electr. Comput. Eng.*, 2015, **38**, (4), pp. 318–322
[116] Madhavan, R., Fernandes, B.G.: 'A novel axial flux segmented SRM for electric vehicle application'. XIX Int. Conf. on Electrical Machines (ICEM), Rome, 2010, pp. 1–6
[117] Lovatt, H.C., Elton, D., Cahill, L., *et al.*: 'Design procedure for low cost, low mass, direct drive, in-wheel motor drivetrains for electric and hybrid vehicles'. IECON 37th Annual Conf. on IEEE Industrial Electronics Society, Melbourne, VIC, 2011, pp. 4558–4562